BER the international journal of bridge engineering management and research

Dynamic Investigations before and after the Strengthening of a Masonry Arch Bridge

Paolo Borlenghi and Carmelo Gentile*

Submitted: 20 August 2025 **Accepted:** 15 September 2025 **Publication date:** 10 October 2025

DOI: 10.70465/ber.v2i4.56

Abstract: The bridge crossing the Gesso River is a multi-span masonry arch bridge built in the 19th century in Cuneo, Piedmont, Italy. Due to extended local degradation and damage, the bridge recently underwent a significant strengthening intervention. Ambient vibration tests were performed both before and after the strengthening to assess the effectiveness of the repairs. The paper presents the results of the dynamic investigations, identifying the modal characteristics of the masonry bridge through different techniques. The pre-intervention analysis revealed clear anomalies, including a sort of "frequency splitting" phenomenon and irregularities in the mode shapes that were localized in the regions of maximum masonry decay. After the strengthening works, the identified modal parameters showed an increase in natural frequencies, along with the resolution of previously identified mode shape irregularities, indicating a clear improvement in the bridge's structural condition.

As a final remark, the presented results highlight the value of operational modal analysis (OMA) as a nondestructive tool for validating the effectiveness of rehabilitation measures.

Author keywords: Historical constructions; rehabilitation; repair; nondestructive testing; operational modal analysis

Introduction

The safety of bridges is a key concern worldwide, and particularly in Italy, where a recent survey documented more than 240 bridge collapses between 2000 and 2023.[1] This evidence highlights the importance of developing effective investigation and rehabilitation strategies for in-service bridges. Within this context, operational modal analysis (OMA) is widely recognized as a powerful tool for the nondestructive assessment of civil engineering structures (see, e.g., Magalhães and Cunha[2]; Rainieri et al.[3]). Generally speaking, OMA consists of estimating the modal characteristics of structures from the dynamic responses measured under operational conditions. The noninvasive nature of OMA, coupled with advances in sensing technologies and the development of numerical methods, has led to its widespread application across various structural typologies and disciplines. Notable examples include the condition assessment of existing bridges[4–8] and footbridges,[9–11] the continuous monitoring of structures for damage identification purposes,[12–14] the development of digital twins for key infrastructures,[15–17] and the evaluation of design choices or future loading scenarios.[18–22]

Despite these advancements, the number of studies applying OMA to evaluate the effectiveness of strengthening interventions remains limited, especially concerning masonry arch bridges. To the best of the authors' knowledge, no published research has specifically addressed the pre- and post-evaluation of the dynamic behavior of a masonry arch bridge using OMA.

Previous studies on reinforced concrete (RC) bridges have shown that the impact of strengthening interventions on dynamic properties can vary significantly according to the structural scheme and the intervention techniques. For instance, Zanardo et al.[23] observed that strengthening a 4-span continuous RC bridge with carbon fiber-reinforced polymer laminate strips resulted in negligible changes (less than 1%) in 2 out of 5 identified natural frequencies, while others showed frequency increases of up to 11%. Similarly, Cury et al.[24] found that additional longitudinal prestressing in a prestressed concrete (PSC) box girder bridge had minimal effects on its modal parameters. Conversely, Cury et al.[25] reported the occurrence of a substantial increase in natural frequencies, up to 15%, following the replacement of elastomeric bearings and expansion joints in a simply supported PSC bridge.

Similarly, research on historical steel bridges[26,27] has shown that structural rehabilitation can lead to a substantial increase in natural frequencies, up to +30%, as well as a significant decrease (–17%), highlighting the crucial role of modal masses.

In masonry structures, the effects of strengthening can be even more significant. For example, Ramos et al.[28] observed

*Corresponding Author: Carmelo Gentile.
Email: carmelo.gentile@polimi.it
Department of Architecture, Built Environment and Construction Engineering (DABC), Politecnico di Milano, Milan, Italy

Discussion period open till six months from the publication date. Please submit separate discussion for each individual paper. This paper is a part of the Vol. 2 of the International Journal of Bridge Engineering, Management and Research (BER), ISSN 3065-0569.

a 50% increase in natural frequencies and a 40% decrease in damping in a masonry tower after rehabilitation works involving lime injection and the installation of ties, likely due to crack closure and the subsequent increase in stiffness. Ercan[29] reported drastic changes in the modal behavior of a stone masonry building after the addition of RC beams at floor levels and the substitution of the roof. Similarly, Namlı and Aras[30] identified substantial increases in modal frequencies—up to 21%—in a masonry school building following the application of RC layers by shotcreting. Conversely, Masciotta et al.[31] found that only limited changes in the modal properties of a historical masonry chimney were induced by the reconstruction of damaged parts and mortar injections, with remarkable variations being observed only for high-frequency local modes.

Given the complexity and variability of masonry structures, evaluating the dynamic response of those structures before and after repair or strengthening is a topic of significant interest. Furthermore, performing an intervention on masonry bridges may be characterized by more constraints compared to buildings, often leading to complex projects being realized without closing the bridge. In this context, OMA is crucial for correctly identifying the pre-intervention structural issues and evaluating whether the solution adopted has been able to solve them (post-intervention). Although several researchers[32–38] have investigated the dynamic characteristics of masonry bridges using OMA, studies specifically addressing the comparison of modal parameters before and after an intervention are still missing.

This paper presents the results of dynamic investigations conducted on a historical multi-span masonry arch bridge, the bridge over the Gesso River in Cuneo, Italy (Figs. 1 and 2), before and after a significant strengthening intervention. The study highlights the retrofit effects by examining the changes in modal parameters. More specifically, a clear increase in natural frequency is observed after the intervention, as well as the disappearance of some mode shapes' anomalies.

The Bridge Over the Gesso River (Cuneo, Italy)

The historic bridge over the Gesso River in Cuneo (Figs. 1 and 2) is one of the two structures that cross the river near the entrance to the historic center of the city. The structure belongs to the Provincial Route SP422 and connects the districts of Borgo San Giuseppe and Cuneo Altopiano. It is managed by the Province of Cuneo, and it is still heavily used by both the traffic in the province and the traffic entering/exiting the densely populated area of the Municipality of Cuneo.

The investigated bridge was built between 1853 and 1856 and is protected by Piedmont's Superintendence of Cultural Heritage. Due to the increased vehicular traffic, a new RC arch bridge was built in 1996 alongside the original structure on the upstream side. The two bridges are independent and share only the base of the piers.

As shown in the geometrical representations in Fig. 2, the bridge under study is approximately 115 m long (including abutments), with a single carriageway 7.30 m wide and two lanes. It consists of three arches with spans of 24 m and two piers placed in the riverbed. The pier height from the foundation level is approximately 10.60 m, and their width along the longitudinal direction is 4.80 m. The piers of the two bridges are connected to each other for the first 6.40 m above the foundation level, while the remaining upper structures are completely independent (this detail is visible in the pictures in Fig. 1).

As known from past inspections, the masonry bridge suffered various decay phenomena, including scouring and common damage due to the aging of the material. Starting in 2018, the Province of Cuneo planned various interventions aimed at solving the observed structural issues. First, measures to prevent riverbed erosion were adopted, whereas the strengthening of the superstructure was subsequently planned. In October 2019, a first series of dynamic tests was performed by the authors to evaluate the modal properties of the structure, highlighting possible critical issues and providing indications for the intervention design.

In preparation for the dynamic tests, visual inspections were performed (Fig. 3). The arch barrels were generally characterized by superficial damage affecting durability, such as black crust, the presence of vegetation, different surface weathering, and diffuse efflorescence. In addition, a severe deterioration of the masonry was localized at the skewback of arch A3 on the side of pier P2 (Fig. 3b).

The strengthening of the bridge (Fig. 4) included the installation of four steel strips at the intrados of each arch barrel, together with the reconstruction of missing masonry portions. Specifically, the local dismantling and reconstruction (often called "scuci-cuci") was applied to fill gaps and restore continuity among damaged masonry portions. In addition, transverse bars were added to connect the external arches with the rest of the arch barrels, ensuring the monolithic behavior of the vaults. Finally, material restoration was carried out using traditional methods, involving cleaning by hydro-washing to remove traces of limestone on the bricks, biocidal treatment to eliminate vegetation, moss, and lichen from masonry surfaces, and protective treatment of decorative stone elements in the form of carved lion heads.

Ambient Vibration Tests and Modal Identification

Ambient vibration tests (AVTs) were performed on October 28th, 2019, and March 4th, 2024, with the main objectives of identifying the dynamic characteristics of the bridge (i.e., natural frequencies, mode shapes, and damping ratios) and assessing their variation after the repair intervention. Notwithstanding the relatively low level of vibration induced by vehicular passages, river flow, wind, and micro-tremors, as well as the high vertical and transverse stiffness of the masonry bridge, AVTs proved to be fully suitable for modal identification.

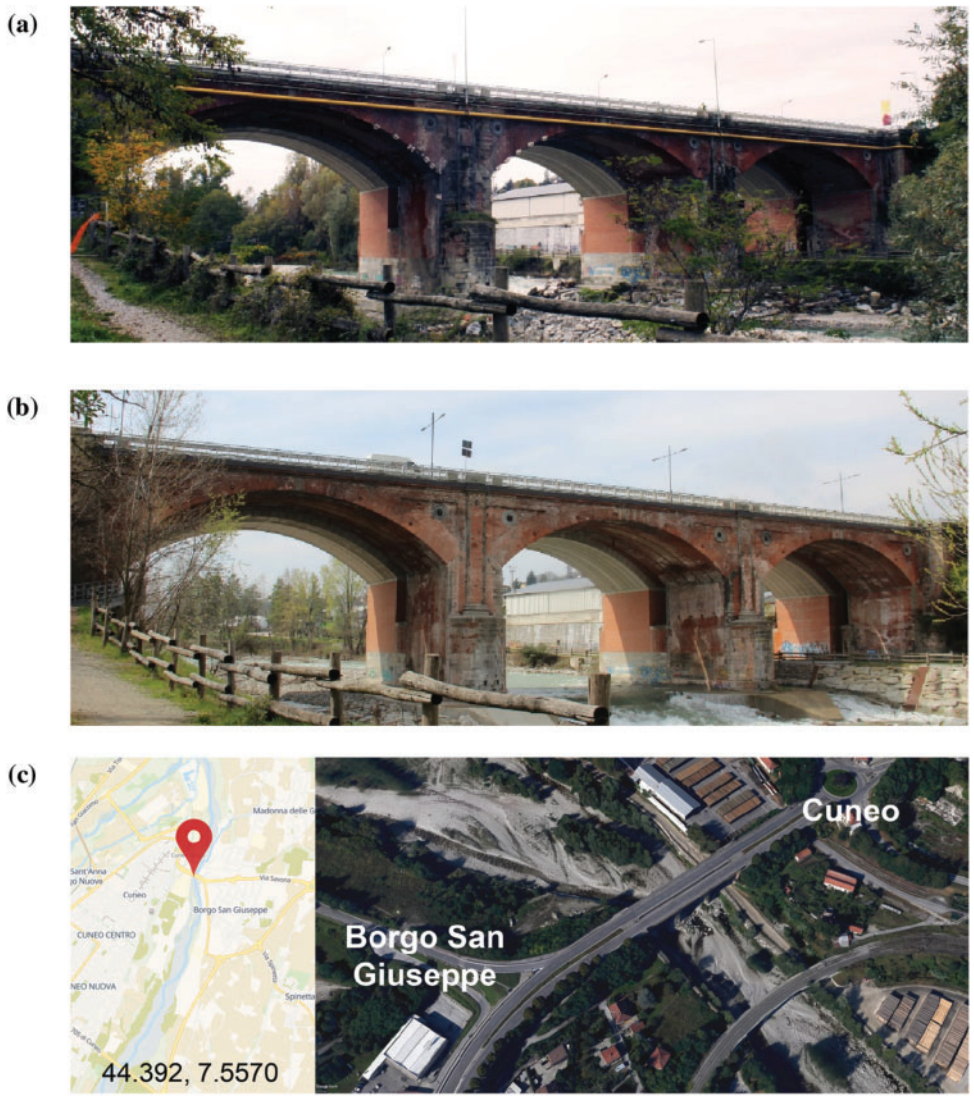

Figure 1. Views from the downstream of the bridge over the Gesso River (Cuneo, Italy) before (a) and after (b) the repair interventions, and (c) bridge location

Experimental procedures

The experimental procedures adopted for the two tests included the measurement of the horizontal and vertical responses of the bridge under operational conditions: due to the presence of sidewalks on both sides, neither traffic interruption nor traffic restrictions were required. Overall, the bridge was instrumented with 17 highly sensitive piezoelectric accelerometers, according to the two measuring setups shown in Fig. 5. The first setup was mainly aimed at characterizing the horizontal response of the structure, with 11 transversal and 6 vertical accelerometers. The second setup was devoted to describing the vertical vibration modes with a higher accuracy, involving 12 vertical and 3 transversal accelerometers. During both setups, 6 vertical (A3, A8, A13, and A15–A17 in Fig. 5) and 3 transversal (A2, A7, and A12 in Fig. 5) accelerometers were used as reference transducers.

The AVTs were conducted using a multichannel acquisition system based on NI9234 devices (24-bit resolution, 102 dB dynamic range, and anti-aliasing filters). The sensors adopted were uniaxial piezoelectric accelerometers (WR model 731A) with 10 V/g sensitivity and ±0.50 g peak acceleration, even though sensors with lower sensitivity could also be suitable. In addition, each sensor was connected to a power unit amplifier (WR model P31) aimed at enhancing the performance of the measuring chain. This unit provided constant current to power the accelerometer's internal amplifier, signal amplification, and selective filtering.

The sampling frequency adopted was equal to 200 Hz, which is more than sufficient for the considered structure, whose dominant frequencies are below 20 Hz. During both tests, the dynamic response of the bridge was recorded for about 90 minutes for each measuring setup.

Data processing and operational modal analysis techniques

The modal identification was performed using the accelerations mainly induced by the regular vehicular traffic on time

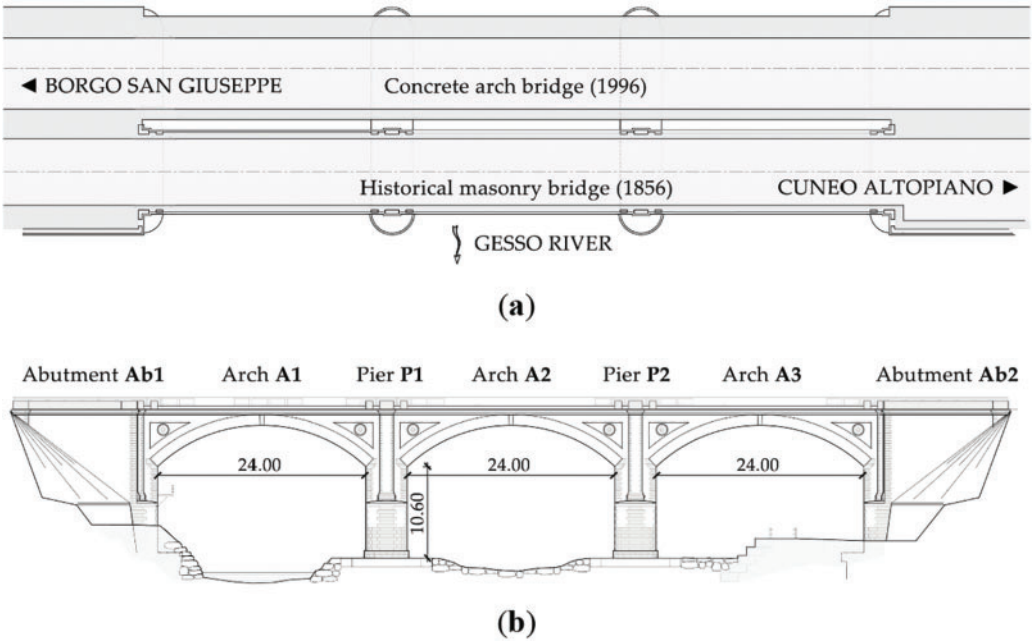

Figure 2. Geometry of the bridge over the Gesso River (Cuneo, Italy): (a) plan and (b) downstream elevation (dimensions in m)

Figure 3. Damages observed at the top of pier P2: (a) general view from downstream and (b) detail of the decayed masonry of the arch A3 skewback (on the right)

Figure 4. Strengthening works: (a) view from downstream of arches A2–A3 and pier P2 and (b) the four steel strips and the transverse connections of the external arch

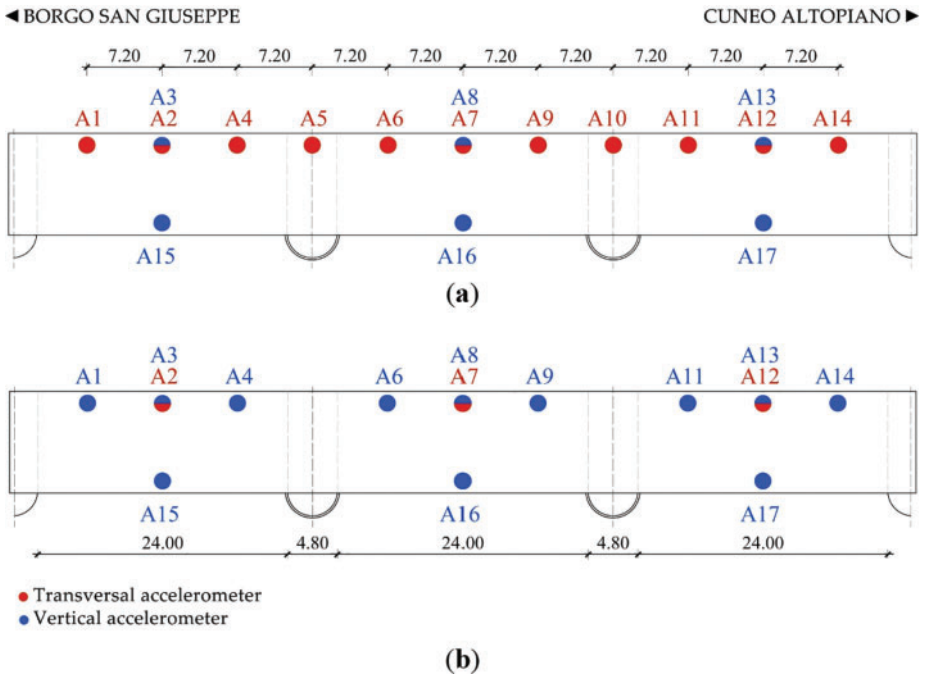

Figure 5. Sensor's layout adopted during the dynamic tests: different configurations to characterize both the transversal (a) and vertical (b) responses

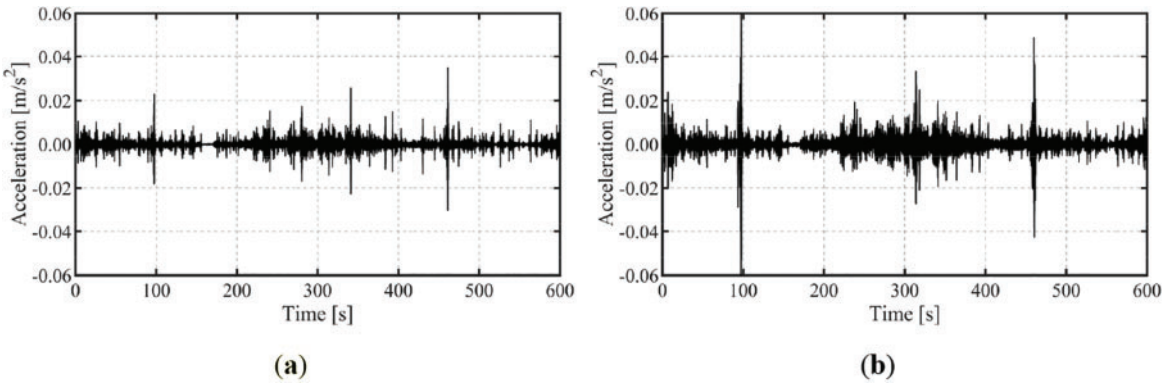

Figure 6. Typical acceleration time series recorded at the center of arch A3 (sensors A12 and A13) in October 2019: (a) lateral and (b) vertical responses

windows of 5400 s. Fig. 6 presents a sample of acceleration time series collected in October 2019, highlighting that the level of vertical vibration is about two times higher (both in terms of RMS and peak accelerations) than that observed in the lateral direction.

From a preliminary modal analysis, it emerged that the vibration modes of the investigated bridge are associated with the dominant vertical or lateral components of motion. Consequently, the modal analysis was performed twice, separating vertical and transverse accelerations. Furthermore, low-pass filtering and decimation were applied to downsample the data to 50 Hz.

In detail, the output-only modal identification was carried out by the frequency domain decomposition (FDD) technique[39] in the frequency domain and the covariance-driven stochastic subspace identification (SSI-Cov) method[40] in the time domain. Both methods have been implemented in MATLAB-based tools developed in previous research.[41]

The FDD technique consists of three main steps: (i) estimation of the spectral matrix **G**; (ii) singular value decomposition (SVD) of **G** at each frequency; (iii) peak-picking of the local maxima in the first singular value curve. The spectral matrix G (containing the auto- and cross-spectra of the responses) is estimated by applying Welch's method[42] to the measured signals. Then, the SVD of **G** is computed at each frequency:

$$\mathbf{G}(f) = \mathbf{U}(f)\boldsymbol{\sigma}(f)\mathbf{U}^{\mathrm{H}}(f) \tag{1}$$

where **U** is a complex matrix containing the singular vectors as columns, the superscript $^{\mathrm{H}}$ denotes a complex conjugate transpose matrix, and $\boldsymbol{\sigma}$ is the diagonal matrix collecting singular values in descending order. At each frequency, the first and largest singular value (σ_1) represents the intensity

of the vibration mode at that frequency. Therefore, the vibration modes can be identified as the local maxima of the first singular value curve: at each selected frequency peak is associated with a mode shape.

The SSI technique is based on the discrete state-space representation of the equations of motion of a linear, time-invariant system subjected to unknown excitation:

$$x_{k+1} = \mathbf{A}\, x_k + w_k \tag{2}$$

$$y_k = \mathbf{C}\, x_k + v_k \tag{3}$$

where $x_k \in \Re^N$ denotes the discrete-time state vector, which includes the displacements and velocities describing the condition of the system at the time instant $t_k = k\Delta t$; $y_k \in \Re^L$ is the output vector, containing the L measured responses; $w_k \in \Re^N$ and $v_k \in \Re^L$ represent the process and measurement noise, respectively. Matrix $\mathbf{A}$ is the discrete state matrix, whose values depend on the structural mass, stiffness, and damping properties, while $\mathbf{C}$ is the discrete output matrix, responsible for mapping the state vector into the measured response. Eq. (2) is commonly referred to as the state equation, whereas Eq. (3) is known as the observation, or output, equation.

In the SSI-Cov method, covariance matrices of the responses are computed at increasing time lags to identify the matrices $\mathbf{A}$ and $\mathbf{C}$ from the recorded signals. These covariance matrices are arranged into a Toeplitz matrix, and then SVD is performed. However, in practical applications, the model order is not known a priori. To address this issue, a common practice is to obtain possible modal parameters by increasing the model order and representing all results in a diagram, called a stabilization diagram. A physical mode is identified when consistent dynamic characteristics (in terms of frequency, damping ratio, and mode shape) are obtained from models of increasing order. Conversely, "modes" or poles characterized by a strong dispersion of modal parameters are called spurious and represent "nonphysical" modes. Cleaning the stabilization diagram, therefore, consists of eliminating spurious poles and identifying stable pole alignments associated with "physical" modes. In detail, the present application adopted the following sequence of cleaning steps: (1) modal damping threshold; (2) mode shape complexity threshold using the modal phase collinearity (MPC) coefficient;[43] and (3) hierarchical clustering. Once the stabilization diagram is cleaned, each cluster is associated with average values of frequency, damping, and mode shape, together with the corresponding standard deviations.

The selection of SSI parameters was guided by the careful interpretation of the stabilization diagrams and prior experience with masonry structures. The chosen time lag (60–70) provided sufficient information to capture the dominant modes while maintaining numerical stability; the model order range (20–120) captured all relevant structural modes while limiting spurious ones; and the damping/MPC thresholds (8–14% and 0.75–0.85) reflected values typically observed in civil structures.[44–46] These criteria, although tuned manually, follow established practice and make the procedure reproducible for future studies.

To compare the mode shapes identified from different methods and tests, the well-known modal assurance criterion (MAC)[47] was computed. The MAC correlation coefficient ranges from 0 to 1: a value greater than 0.85 indicates a good correlation, whereas a value lower than 0.50 is considered a poor match.

Dynamic Characteristics of the Bridge Over the Gesso River

Dynamic characteristics before strengthening (October 2019)

As previously pointed out, the first AVT was carried out in late October 2019, during daytime, with air temperature ranging between 16.5°C and 17.6°C. The application of FDD and SSI techniques led to the identification of 5 lateral and 3 vertical vibration modes in the frequency range of 0–18 Hz.

As shown in Fig. 7, the vibration modes are identified from the local maxima of the first SV line using the FDD method (Fig. 7a refers to lateral responses, whereas Fig. 7b relates to the vertical ones) and through the alignment of stable poles in the stabilization diagram obtained by applying the SSI method (Fig. 7c refers to lateral responses and Fig. 7d to vertical ones). As expected, the spectral analysis of vertical accelerations exhibits more evident peaks due to the higher excitation level. Nevertheless, both methods provided consistent indications of the same vibration modes in both lateral and vertical responses.

Fig. 8 shows the mode shapes identified using the FDD method. The fundamental vibration mode is in the transverse direction, and with a frequency of 5.3 Hz. The lateral modes exhibit an increasing number of half-sine waves and inflection points, with the only exception being mode L3*, which has the same mode shape as mode L3. The mode shapes V1 and V2 are associated with vertical bending, while V3 corresponds to a torsional mode.

Table 1 summarizes the results obtained by applying the FDD and the SSI identification methods through: (a) the natural frequencies identified by the FDD technique; (b) the natural frequencies and modal damping ratios identified by the SSI method. In addition, Table 1 compares the estimates of corresponding mode shapes obtained by the two techniques through the MAC. The limited differences in mode shapes are demonstrated by a MAC larger than 0.90 for all modes except for L3*, for which the MAC is equal to 0.84. In this last case, the FDD technique seems to provide a more accurate estimation of the mode shape.

The modal characteristics identified in the first test suggest the following comments:

- The damping estimates are generally relatively high, with modes L1, L2, and L4 having values higher than 7%.
- Modes L1 and L2 exhibit a local distortion of the mode shapes, localized at the third quarter of arch A1 (Borgo side) and–more evidently–at the first quarter of arch A3 (Cuneo side). As highlighted by visual

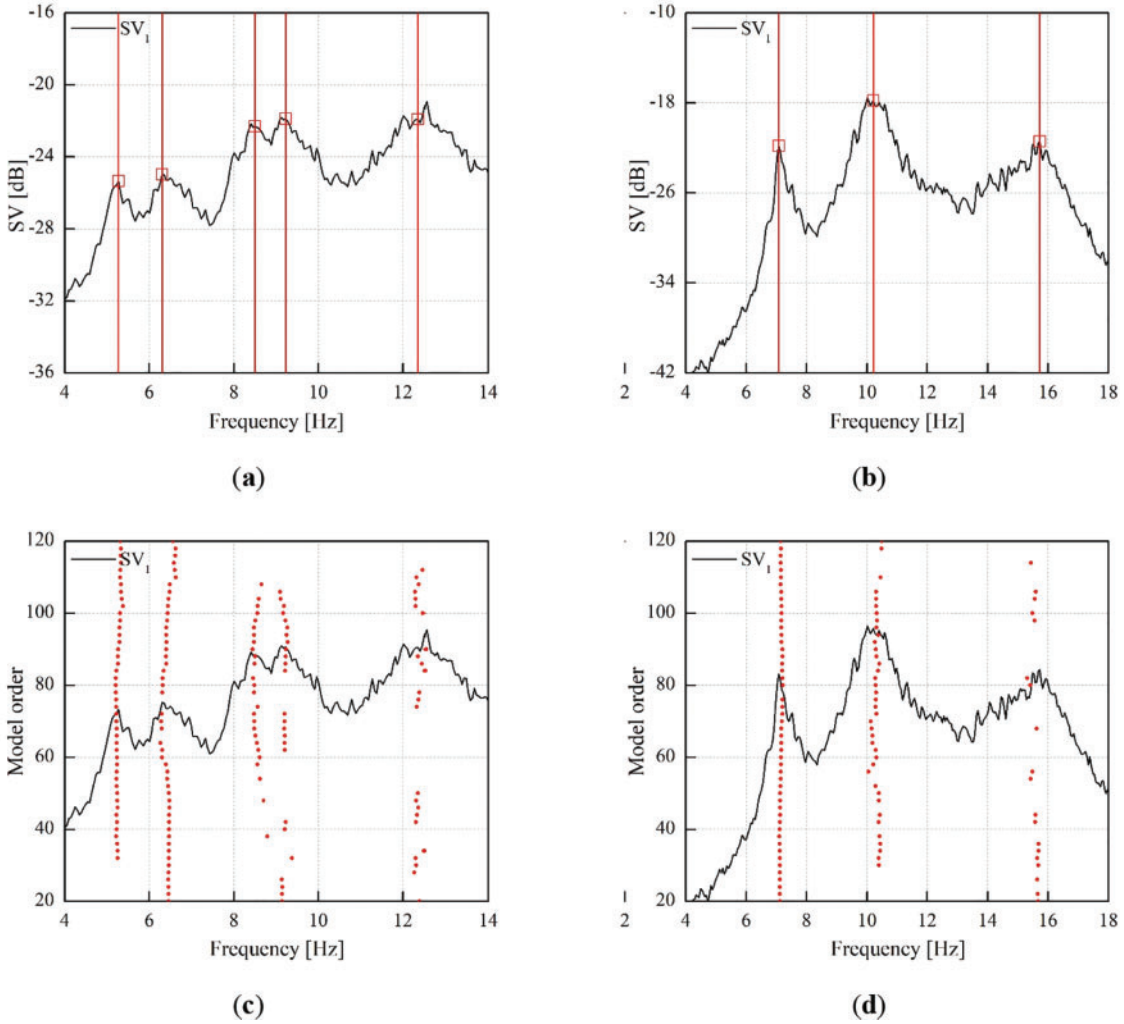

Figure 7. Identification of vibration modes from the AVT of October 2019: (a, b) first singular value (SV) curve and peak picking (FDD) of horizontal and vertical accelerations, respectively; (c, d) stabilization diagram (SSI-Cov) of horizontal and vertical accelerations, respectively

inspection, the arch barrels are affected in those regions by a severe state of degradation, providing a possible explanation for the identified irregularities.

- Mode L3* exhibits the same mode shape as mode L3 with a slight difference in natural frequency. This phenomenon should be classified as a "frequency splitting"[48] and, in this case, it is likely related to existing damage at the arch barrels, although this remains an assumption supported by indirect evidence. Particularly, the visual inspections highlighted the presence of discontinuities at the skewback between arch A3 and pier P2, where mode L3 exhibits the maximum modal displacement.

Dynamic characteristics after strengthening (March 2024)

The second AVT was performed at the beginning of March 2024, during daytime, with air temperature ranging between 12.8°C and 16.9°C. Applying the FDD and SSI techniques led to the identification of 7 vibration modes in the frequency range of 0–18 Hz: 4 lateral and 3 vertical modes.

The output-only identification was first performed with the FDD technique: Figs. 9a, 9b shows the first SV line obtained from the analysis of the lateral and vertical accelerations, respectively. As shown by the alignments of stable poles in Figs. 9c, 9d, the SSI-Cov algorithm was also applied to lateral and vertical responses, respectively. It should be noted that the presence of normal modes is clearly highlighted by both the local maxima of the SV lines (FDD) and the corresponding alignments of stable poles (SSI-Cov).

Fig. 10 illustrates the mode shapes identified by applying the FDD method. The fundamental vibration mode is characterized by a predominant transverse modal displacement with a natural frequency of 5.8 Hz. The subsequent lateral modes exhibit an increasing number of half-sine waves and inflection points, as expected. Furthermore, vibration modes V1 and V2 are associated with vertical bending, while mode V3 represents a vertical torsion mode.

Table 2 summarizes the natural frequencies identified by applying the FDD and SSI-Cov procedures, the damping

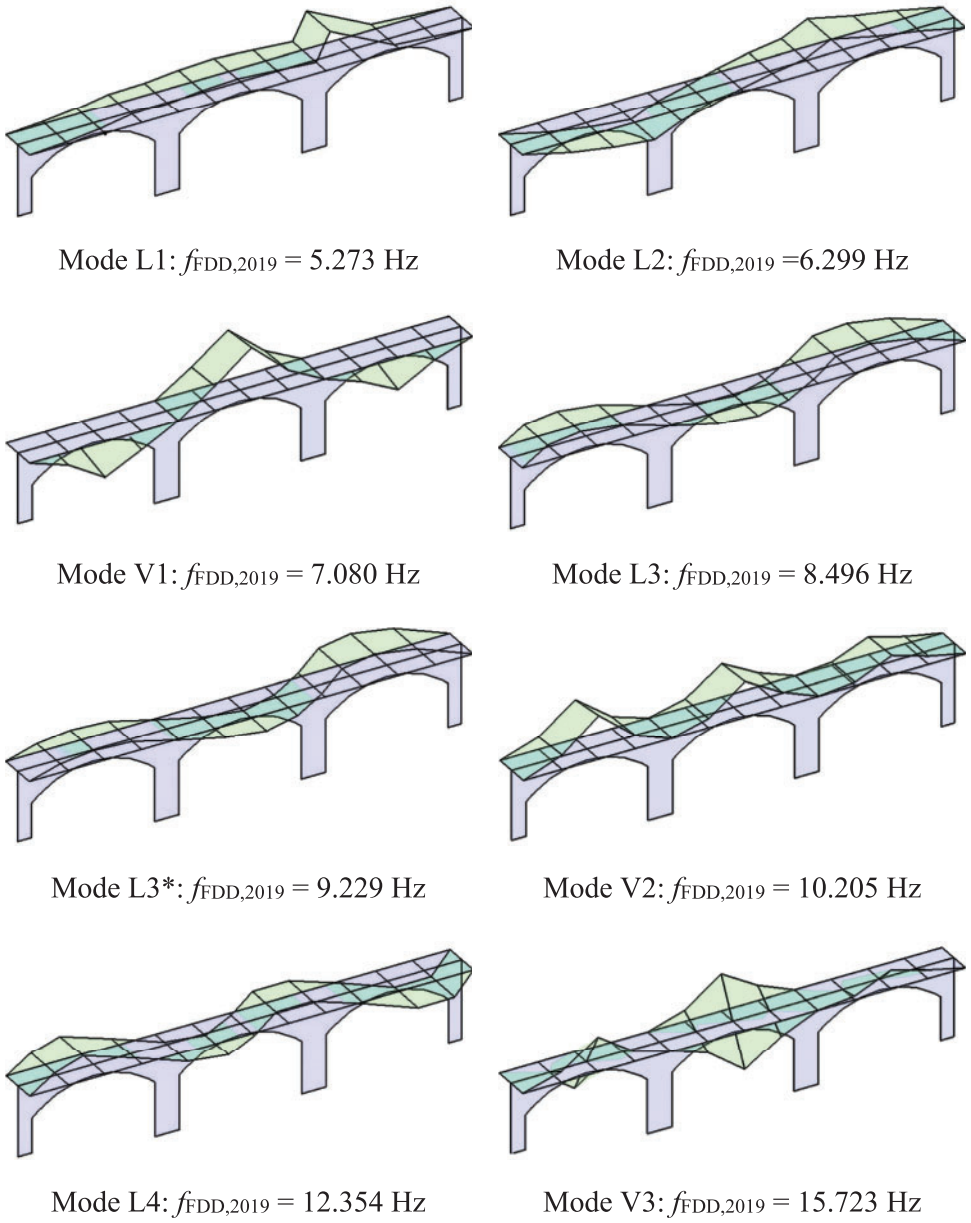

Figure 8. Vibration modes identified before the repair intervention in October 2019 (L = dominant lateral, V = dominant vertical)

Table 1. Summary of the modal parameters identified in 2019 by FDD and SSI

Mode ID	FDD	SSI		MAC
	f_{2019} (Hz)	f_{2019} (Hz)	ζ (%)	
L1	5.273	5.263	7.65	0.97
L2	6.299	6.435	7.47	0.96
V1	7.080	7.154	3.36	0.99
L3	8.496	8.541	2.98	0.94
L3*	9.229	9.204	4.97	0.84
V2	10.205	10.321	2.54	0.98
L4	12.354	12.371	7.84	0.96
V3	15.723	15.563	3.11	0.92

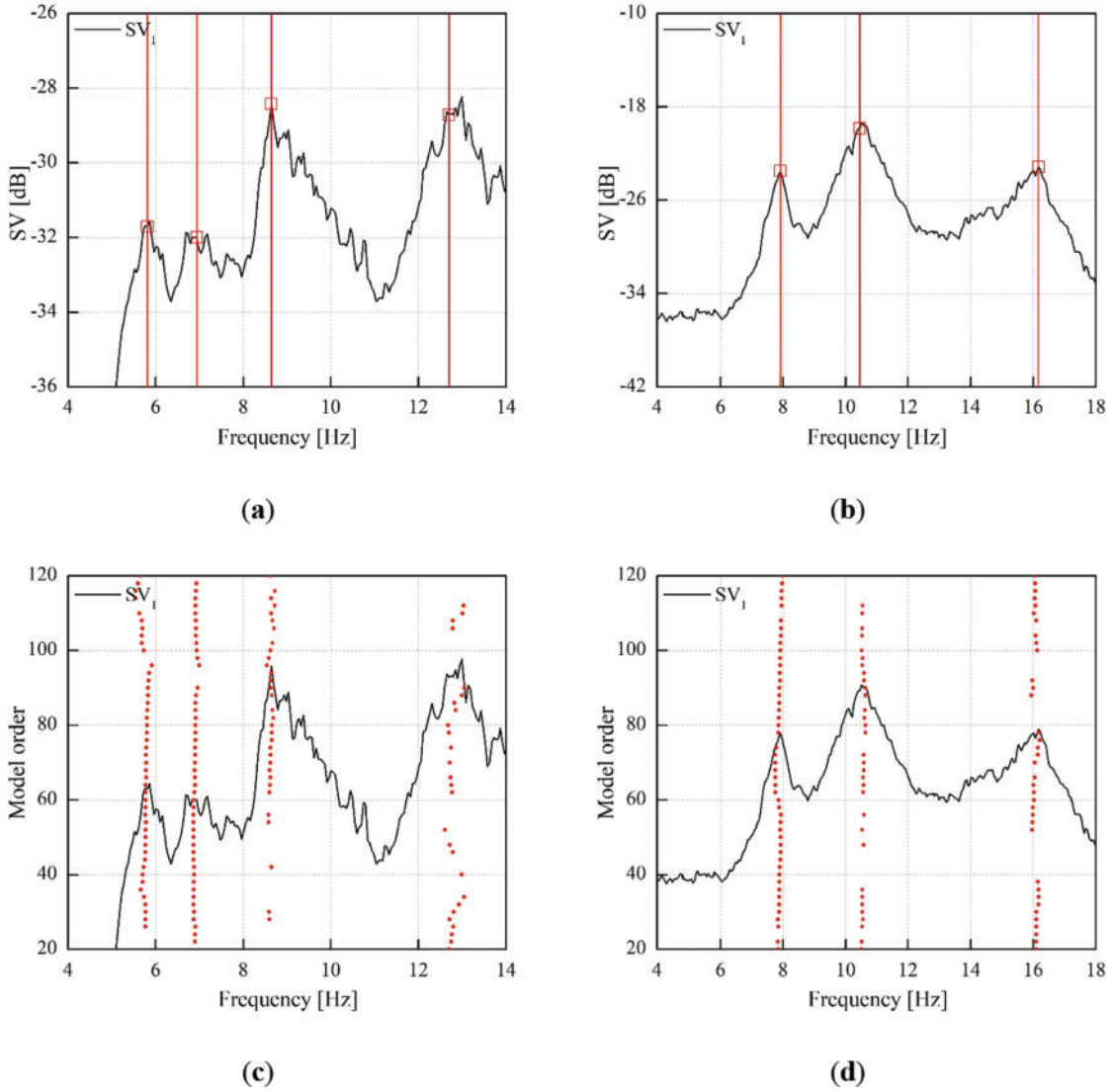

Figure 9. Identification of vibration modes from the AVT of March 2024: (a, b) first singular value curve and peak picking (FDD) of horizontal and vertical accelerations, respectively; (c, d) stabilization diagram (SSI-Cov) of horizontal and vertical accelerations, respectively

ratios (from SSI-Cov), and the MAC between the corresponding mode shapes. The differences in mode shapes are generally negligible, with MAC values greater than 0.98 for the first four modes and values ranging from 0.92 to 0.96 for the higher modes.

The modal characteristics identified in the second test suggest the following comments:

- The estimates of modal damping are particularly high for modes L1 and L2, with values greater than 9%, while for the other modes, the damping ranges from a minimum of 3% for mode V3 to a maximum of 5.6% for mode L4.
- The mode shapes are generally regular but not perfectly symmetrical with respect to the center of the structure. This is particularly visible in the mode shapes L2 and L4, in which the modal displacements at piers P1 and P2 are nonsymmetric.

Comparison between the Modal Properties before and after the Intervention

Performing dynamic investigations before and after the strengthening intervention allowed the evaluation of the intervention's effects in solving the detected structural issues. The AVT carried out after the consolidation works was indeed a substantial repetition of the 2019 investigation, employing the same measurement devices and the same measurement positions.

During the 2024 test, seven vibration modes were identified, while in the 2019 test, an additional vibration mode was present. As previously noted, the additional vibration mode L3* is probably related to the "frequency splitting" phenomenon generated by the presence of discontinuities at the skewback between arch A3 and pier P2. The absence of mode L3* in the 2024 results suggests the effectiveness

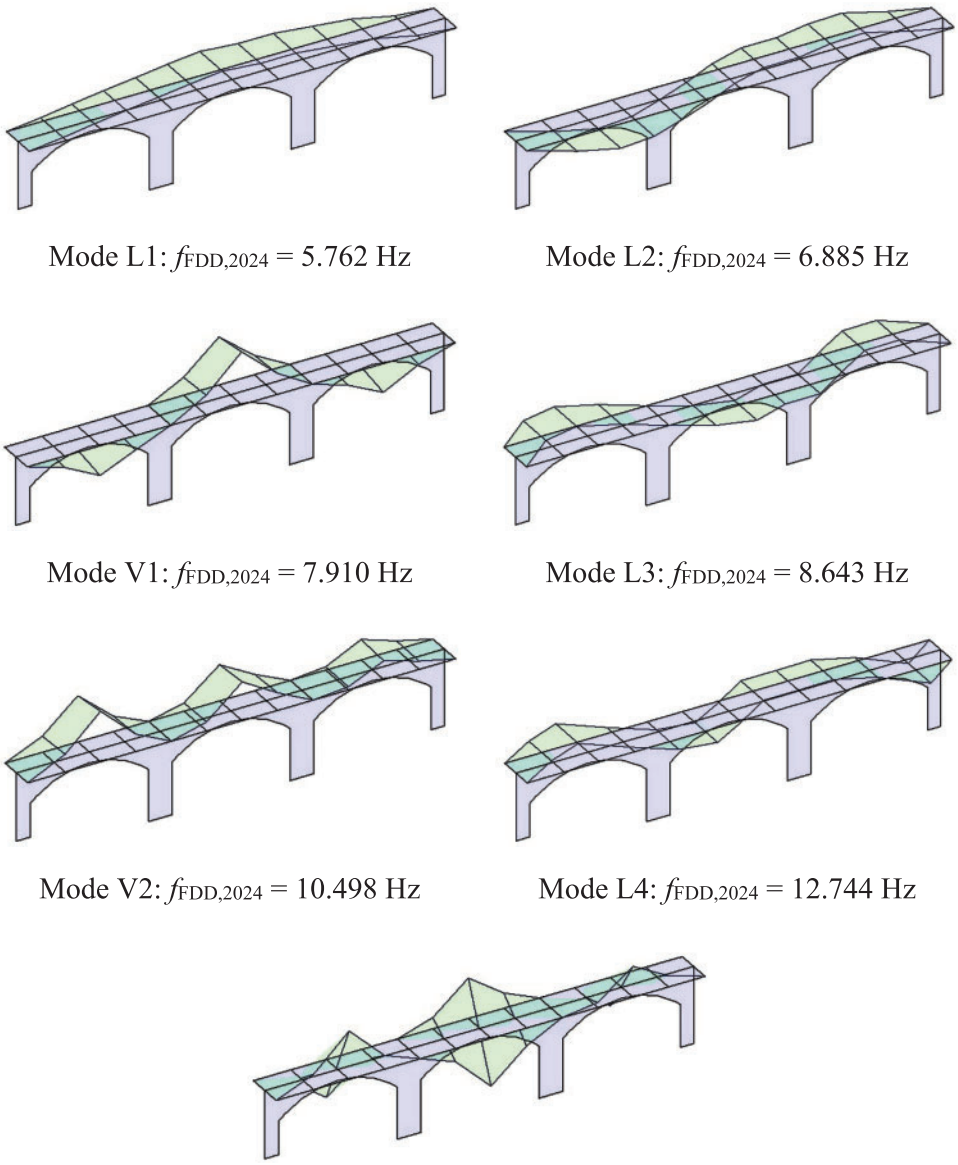

Figure 10. Vibration modes identified after the repair intervention in March 2024 (L = dominant lateral, V = dominant vertical)

Table 2. Summary of the modal parameters identified in 2024 by FDD and SSI

Mode ID	FDD	SSI		MAC
	f_{2024} (Hz)	f_{2024} (Hz)	ζ (%)	
L1	5.762	5.751	10.66	1.00
L2	6.885	6.898	9.62	0.99
V1	7.910	7.878	3.85	0.99
L3	8.643	8.632	4.71	0.98
V2	10.498	10.562	3.78	0.92
L4	12.744	12.814	5.64	0.92
V3	16.162	16.069	3.26	0.96

Table 3. Comparison between the natural frequencies identified in 2024 and 2019

Mode ID	$f_{FDD,2019}$ (Hz)	$f_{FDD,2024}$ (Hz)	Δf (%)
L1	5.273	5.762	+9.27
L2	6.299	6.885	+9.30
V1	7.080	7.910	+11.7
L3	8.496	8.643	+1.73
V2	10.205	10.498	+2.84
L4	12.354	12.744	+3.16
V3	15.723	16.162	+2.80

$\Delta f = [(f_{FDD,2024}/f_{FDD,2019}) - 1] \times 100$

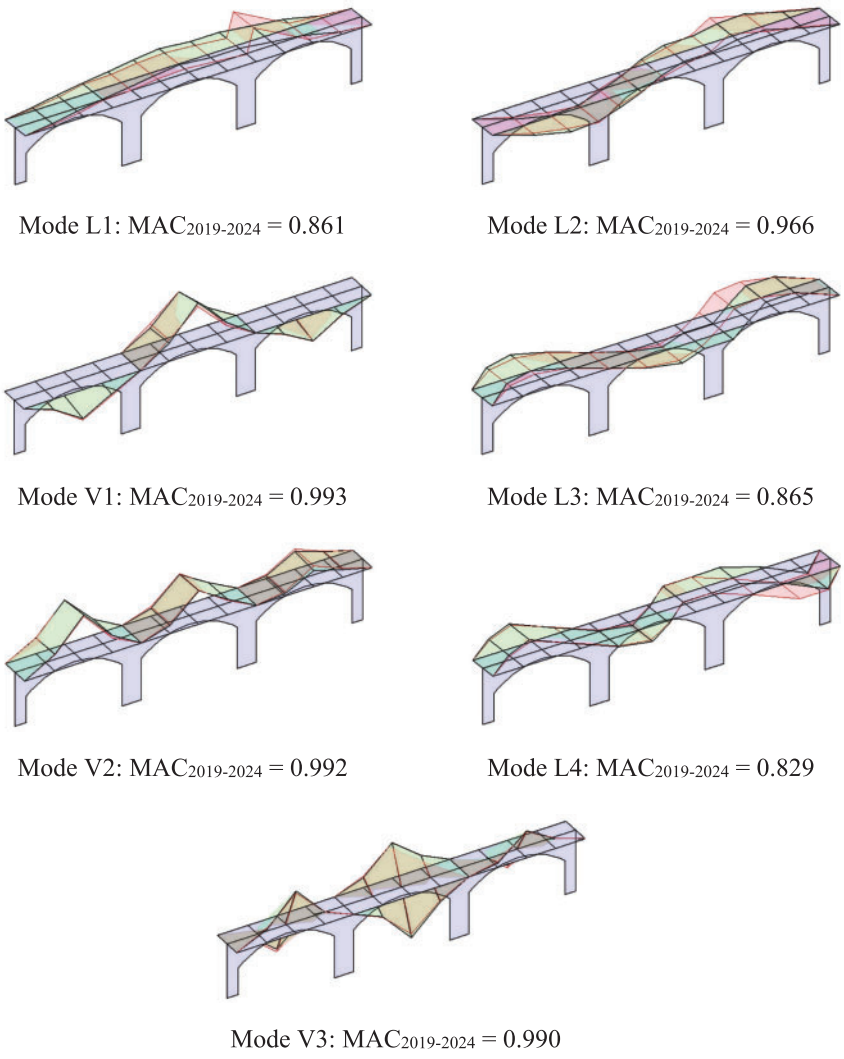

Figure 11. Comparison between the vibration modes identified in 2019 and 2024

of the intervention in repairing the existing damages and discontinuities.

Table 3 and Fig. 11 illustrate the comparison between the current dynamic characteristics (2024) and those identified in 2019 using the FDD method. In particular, Table 3 shows a substantial increase in natural frequencies, with an average percentage value across the seven modes of +5.4%, and a more pronounced increase in the first three modes (L1, L2, and V1), with an average percentage value of +9.2%.

The average temperatures recorded during the two surveys were 17.1°C and 15.0°C on October 28, 2019 and April 4, 2024, respectively. As known from previous monitoring experiences on masonry structures,[12,14] natural frequencies tend to increase with temperature increase. Consequently, the slight decrease in temperature between the 2019 and 2024

tests should have caused a slight reduction in natural frequencies rather than contributing to the identified increase. In other words, the observed frequency increase might be even higher once the temperature effects are compensated.

Regarding the other environmental and operational effects, both tests were conducted under moderate vehicular traffic conditions, with an average flow of light vehicles and occasional heavy trucks. The river level was close to the seasonal average, and weather conditions were stable. These conditions were comparable between the two surveys and, as expected, no effects on the identified dynamic behavior were observed.

Fig. 11 presents a comparison of the mode shapes with the associated MAC factor. The consistently high MAC correlation factors confirm that the nature of the modes identified in the two tests is the same, with values exceeding 0.8. However, the comparison reveals localized differences in the modal deformations before and after the intervention. In the 2019 test, irregularities were found in the modal deformations at measurement points A4 (third quarter of the lateral arch on the Borgo S. Giuseppe side) and, more prominently, A11 (first quarter of the lateral arch on the Cuneo Altopiano side). In the 2024 investigations, the previously observed distortions appear to have been effectively resolved, suggesting a clear improvement in the bridge's condition.

Conclusions

The paper focuses on the operational modal analysis of a historical masonry arch bridge (1856) to evaluate the effectiveness of a strengthening intervention. Two dynamic tests under operational conditions were carried out before and after the repair work (in October 2019 and April 2024, respectively). The dynamic characteristics of the structure were evaluated using the FDD and SSI-Cov output-only identification techniques.

The visual inspections carried out in 2019 revealed the general state of degradation of the brick masonry and the presence of a severe discontinuity at the skewback between arch A3 and pier P2. The OMA highlighted irregularities in the mode shapes, which were more evident around the structural discontinuity. In addition, the presence of two vibration modes characterized by a slight difference in natural frequencies but the same mode shape (i.e., L3 and L3*) suggests the presence of a "frequency splitting" phenomenon caused—again—by the discontinuity at pier P2–arch A3.

Following the strengthening intervention, the 2024 test indicated a clear change in the bridge's dynamic response. The disappearance of mode L3* and the remarkable increase in natural frequencies, particularly in the first three modes, demonstrated the success of the repairs in addressing the previously identified damages. In addition, the comparison of mode shapes before and after the intervention, supported by a consistently high MAC correlation factor, further confirmed the structural improvements, with the irregularities in modal displacements being effectively amended.

Overall, the results presented show that operational modal testing and analysis are effective tools for evaluating the dynamic behavior of masonry bridges. These methods provide valuable insights for assessing structural deficiencies and evaluating the effectiveness of strengthening interventions. Future developments of this research will focus on collecting additional information on the bridge geometry, material properties, and details of the strengthening works. These data will enable the development of a calibrated numerical model, which will be used to support a quantitative assessment of the damage and to complement the experimental results presented in this study.

Acknowledgments

Sincere thanks are due to M. Cucchi, M. Iscandri (LPMSC, Politecnico di Milano), and PhD A. Ruccolo (DABC, Politecnico di Milano), for their assistance in conducting the field tests.

Author Contributions

Conceptualization, P.B. and C.G.; investigation, P.B. and C.G.; data curation, P.B. and C.G.; writing—original draft preparation, P.B.; writing—review and editing, P.B. and C.G.; visualization, P.B.; supervision, C.G.; funding acquisition, C.G. All authors have read and agreed to the published version of the manuscript.

Data Availability Statement

The experimental datasets collected and analyzed during the current study are available from the corresponding author upon reasonable request. Additionally, data requests will require approval from the bridge manager (Province of Cuneo).

Conflicts of Interest

The authors declare no conflicts of interest.

References

[1] D'Angelo M, Civera M, Giordano PF, et al. Bridge collapses in Italy across the 21st century: survey and statistical analysis. *Struct Infrastruct Eng*. 2025. doi:10.1080/15732479.2025.2483500.

[2] Magalhães F, Cunha A. Explaining operational modal analysis with data from an arch bridge. *Mech Syst Signal Process*. 2011;25(5):1431–1450. doi:10.1016/j.ymssp.2010.08.001.

[3] Rainieri C, Notarangelo MA, Fabbrocino G. Experiences of dynamic identification and monitoring of bridges in serviceability conditions and after hazardous events. *Infrastructures (Basel)*. 2020;5(10):1–23. doi:10.3390/infrastructures5100086.

[4] Benedettini F, Dilena M, Morassi A. Vibration analysis and structural identification of a curved multi-span

viaduct. *Mech Syst Signal Process*. 2015;54(12):84–107. doi:10.1016/j.ymssp.2014.08.008.

[5] Clemente P, Bongiovanni G, Buffarini G, Saitta F. Structural health status assessment of a cable-stayed bridge by means of experimental vibration analysis. *J Civ Struct Health Monit*. 2019;9(5):655–669. doi:10.1007/s13349-019-00359-2.

[6] Cunha Á, Caetano E, Magalhães F, Moutinho C. Dynamic identification and continuous dynamic monitoring of bridges: different applications along bridges life cycle. *Struct Infrastruct Eng*. 2018;14(4):445–467. doi:10.1080/15732479.2017.1406959.

[7] D'angelo M, Menghini A, Borlenghi P, et al. Hydraulic safety evaluation and dynamic investigations of Baghetto Bridge in Italy. *Infrastructures (Basel)*. 2022;7(4):53. doi:10.3390/infrastructures7040053.

[8] Gentile C, Saisi A. Ambient vibration testing and condition assessment of the Paderno iron arch bridge. *1889 Constr Build Mater*. 2011;25(9):3709–3720. doi:10.1016/j.conbuildmat.2011.04.019.

[9] Bayat E, Milone A, Tubino F, Venuti F. Vibration serviceability assessment of a historic suspension footbridge. *Buildings*. 2022;12(6):732. doi:10.3390/buildings12060732.

[10] Caetano E, Cunha Á, Magalhães F, Moutinho C. Studies for controlling human-induced vibration of the Pedro e Inês footbridge, Portugal. Part 1: assessment of dynamic behaviour. *Eng Struct*. 2010;32(4):1069–1081. doi:10.1016/j.engstruct.2009.12.034.

[11] Nicoletti V, Quarchioni S, Tentella L, Martini R, Gara F. Experimental tests and numerical analyses for the dynamic characterization of a steel and wooden cable-stayed footbridge. *Infrastructures (Basel)*. 2023b;8(6):100. doi:10.3390/infrastructures8060100.

[12] Gentile C, Guidobaldi M, Saisi A. One-year dynamic monitoring of a historic tower: damage detection under changing environment. *Meccanica*. 2016;51(11):2873–2889. doi:10.1007/s11012-016-0482-3.

[13] Magalhães F, Cunha A, Caetano E. Online automatic identification of the modal parameters of a long span arch bridge. *Mech Syst Signal Process*. 2009;23(2):316–329. doi:10.1016/j.ymssp.2008.05.003.

[14] Ubertini F, Cavalagli N, Kita A, Comanducci G. Assessment of a monumental masonry bell-tower after 2016 central Italy seismic sequence by long-term SHM. *Bullet Earthq Eng*. 2018;16(2):775–801. doi:10.1007/s10518-017-0222-7.

[15] Catbas FN, Cano JA, Luleci F, Walters LC, Michlowitz R. On the generation of digital data and models from point clouds: application to a pedestrian bridge structure. *Infrastructures (Basel)*. 2024;9(1):6. doi:10.3390/infrastructures9010006.

[16] Funari MF, Hajjat AE, Masciotta MG, Oliveira DV, Lourenço PB. A parametric scan-to-FEM framework for the digital twin generation of historic masonry structures. *Sustainability (Switzerland)*. 2021;13(19):11088. doi:10.3390/su131911088.

[17] Nicoletti V, Martini R, Carbonari S, Gara F. Operational modal analysis as a support for the development of digital twin models of bridges. *Infrastructures (Basel)*. 2023a;8(2):24. doi:10.3390/infrastructures8020024.

[18] Brownjohn JMW, Moyo P, Omenzetter P, Lu Y. Assessment of highway bridge upgrading by dynamic testing and finite-element model updating. *J Bridge Eng*. 2003;8:3–162. doi:10.1061/(asce)1084-0702(2003)8:3(162).

[19] Castelli S, Labò S, Belleri A, Moaveni B. Operational modal analysis, seismic vulnerability assessment and retrofit of a degraded RC bell tower. *J Civ Struct Health Monit*. 2024;14(4):885–907. doi:10.1007/s13349-024-00765-1.

[20] Pierdicca A, Clementi F, Fortunati A, Lenci S. Tracking modal parameters evolution of a school building during retrofitting works. *Bullet Earthquake Eng*. 2019;17(2):1029–1052. doi:10.1007/s10518-018-0483-9.

[21] Ribeiro D, Costa B, Cruz L, et al. Simulation of the dynamic behavior of a centenary metallic bridge under metro traffic actions based on advanced interaction models. *Int J Struct Stab Dynam*. 2021;21(04):2150057. doi:10.1142/S0219455421500577.

[22] Zaki MA, Abu-Hamd MH. Rehabilitation assessment of a steel railway bridge by dynamic field testing. *Struct Infrastruct Eng*. 2007;3(4):343–353. doi:10.1080/15732470600578767.

[23] Zanardo G, Hao H, Xia Y, Deeks AJ. Stiffness assessment through modal analysis of an RC slab bridge before and after strengthening. *J Bridge Eng*. 2006;11:590–601. doi:10.1061/(ASCE)1084-0702(2006)11:5(590).

[24] Cury A, Cremona C, Dumoulin J. Long-term monitoring of a PSC box girder bridge: operational modal analysis, data normalization and structural modification assessment. *Mech Syst Signal Process*. 2012;33:13–37. doi:10.1016/j.ymssp.2012.07.005.

[25] Maalek S, Akbari R, Ziaei-Rad S. The effects of the repair operations and replacement of the elastomeric bearings on the modal characteristics of a highway bridge. *Struct Infrastruct Eng*. 2010;6(6):753–765. doi:10.1080/15732470802334829.

[26] Costa BJA, Magalhães F, Cunha T, Figueiras J. Rehabilitation assessment of a centenary steel bridge based on modal analysis. *Eng Struct*. 2013;56(4):260–272. doi:10.1016/j.engstruct.2013.05.010.

[27] Costa BJA, Magalhães F, Cunha Á, Figueiras J. Modal analysis for the rehabilitation assessment of the Luiz I Bridge. *J Bridge Eng*. 2014;19(12):14. doi:10.1061/(ASCE)BE.1943-5592.0000632.

[28] Ramos LF, Marques L, Lourenço PB, De Roeck G, Campos-Costa A, Roque J. Monitoring historical masonry structures with operational modal analysis: two case studies. *Mech Syst Signal Process*. 2010;24(5):1291–1305. doi:10.1016/j.ymssp.2010.01.011.

[29] Ercan E. Assessing the impact of retrofitting on structural safety in historical buildings via ambient vibration tests. *Constr Build Mater*. 2018;164(1):337–349. doi:10.1016/j.conbuildmat.2017.12.154.

[30] Namlı M, Aras F. Performance evaluation of a seismic strengthening applied on a masonry school building by dynamic analyses. *Structures*. 2024;62(2):106200. doi:10.1016/j.istruc.2024.106200.

[31] Masciotta M-G, Ramos LF, Lourenço PB, Vasta M. Damage identification and seismic vulnerability assessment of a historic masonry chimney. *Ann Geophy*. 2017;60(4):S0442. doi:10.4401/ag-7126.

[32] Borlenghi P, Saisi A, Gentile C. ND testing and establishing models of a multi-span masonry arch bridge. *J Civ Struct Health Monit*. 2023;13(8):1595–1611. doi:10.1007/s13349-022-00666-1.

[33] Brencich A, Sabia D. Experimental identification of a multi-span masonry bridge: the Tanaro Bridge. *Constr Build Mater*. 2008;22(10):2087–2099. doi:10.1016/j.conbuildmat.2007.07.031.

[34] Civera M, Mugnaini V, Zanotti Fragonara L. Machine learning-based automatic operational modal analysis: a structural health monitoring application to masonry arch

bridges. *Struct Control Health Monit*. 2022;29(10):499. doi:10.1002/stc.3028.
[35] Costa C, Ribeiro D, Jorge P, Silva R, Arêde A, Calçada R. Calibration of the numerical model of a stone masonry railway bridge based on experimentally identified modal parameters. *Eng Struct*. 2016;123(2):354–371. doi:10.1016/j.engstruct.2016.05.044.
[36] Mansour S, Rizzo F, Giannoccaro NI, La Scala A, Sabbà MF, Foti D. Essential dynamic characterization of a historical bridge: integrated experimental and numerical investigations. *J Civ Struct Health Monit*. 2024;14(1):85–102. doi:10.1007/s13349-023-00744-y.
[37] Pantò B, Ortega J, Grosman S, et al. Advanced calibration of a 3D masonry arch bridge model using non-destructive testing and numerical optimisation. *Constr Build Mater*. 2024;438(5):137131. doi:10.1016/j.conbuildmat.2024.137131.
[38] Zini G, Betti M, Bartoli G, Morano SG, Spinelli P. Structural health monitoring of a masonry arch bridge: modal identification and model updating. *Int J Maso Res Innovat*. 2023;9(1/2):42–53. doi:10.1504/IJMRI.2024.135244.
[39] Brincker R, Zhang L, Andersen P. Modal identification of output-only systems using frequency domain decomposition. *Smart Mater Struct*. 2001;10(3):441–445. doi:10.1088/0964-1726/10/3/303.
[40] Peeters B, De Roeck G. Reference-based stochastic subspace identification for output-only modal analysis. *Mech Syst Signal Process*. 1999;13(6):855–878. doi:10.1006/mssp.1999.1249.
[41] Gentile C, Pirrò M, Borlenghi P. DYMOND: a matlab toolbox for the dynamic monitoring of bridges according to the Lombardia regional guidelines. *Lect Not Civil Eng*. 2024;514 LNCE:476–487. doi:10.1007/978-3-031-61421-7_47.
[42] Welch PD. The use of fast fourier transform for the estimation of power spectra: a method based on time averaging over short, modified periodograms. *IEEE Transact Aud Electroacou*. 1967;15(2):70–73. doi:10.1109/TAU.1967.1161901.
[43] Pappa RS, Elliott KB, Schenk A. Consistent-mode indicator for the eigensystem realization algorithm. *J Guid Cont Dynam*. 1993;16(5):852–858. doi:10.2514/3.21092.
[44] Anastasopoulos D, Reynders EPB. Modal strain monitoring of the old Nieuwebrugstraat Bridge: local damage versus temperature effects. *Eng Struct*. 2023;296(3–4):116854. doi:10.1016/j.engstruct.2023.116854.
[45] Cabboi A, Gentile C, Saisi A. From continuous vibration monitoring to FEM-based damage assessment: application on a stone-masonry tower. *Constr Build Mater*. 2017;156(5):252–265. doi:10.1016/j.conbuildmat.2017.08.160.
[46] Hernández-González IA, García-Macías E, Costante G, Ubertini F. AI-driven blind source separation for fast operational modal analysis of structures. *Mech Syst Signal Process*. 2024;211(5):111267. doi:10.1016/j.ymssp.2024.111267.
[47] Allemang RJ, Brown DL. Correlation coefficient for modal vector analysis. *Proceedings of the International Modal Analysis Conference & Exhibit*; 1982
[48] Zonta D, Modena C. Observations on the appearance of dispersive phenomena in damaged structures. *J Sound Vib*. 2001;241(5):925–933. doi:10.1006/jsvi.2000.3320.